Separation Science and Technology
Publication details, including instructions for authors and subscription information:
http://www.informaworld.com/smpp/title~content=t713708471

Removal of Fluoride from Aqueous Solution by CaO Nanoparticles

Gaurang Patel[a]; Usha Pal[a]; Shobhana Menon[a]
[a] Department of Chemistry, School of Sciences, Gujarat University, Ahmedabad, Gujarat, India

To cite this Article Patel, Gaurang , Pal, Usha and Menon, Shobhana(2009) 'Removal of Fluoride from Aqueous Solution by CaO Nanoparticles', Separation Science and Technology, 44: 12, 2806 — 2826
To link to this Article: DOI: 10.1080/01496390903014425
URL: http://dx.doi.org/10.1080/01496390903014425

Separation Science and Technology, 44: 2806–2826, 2009

ISSN: 0149-6395 print/1520-5754 online
DOI: 10.1080/01496390903014425

Taylor & Francis
Taylor & Francis Group

Removal of Fluoride from Aqueous Solution by CaO Nanoparticles

Gaurang Patel, Usha Pal, and Shobhana Menon
Department of Chemistry, School of Sciences, Gujarat University, Ahmedabad, Gujarat, India

Abstract: Colloidal particles of CaO were synthesized by the sol-gel method. The particle morphology was characterized by FT-IR, TGA, DTA, and TEM analysis. The ability of the CaO nanoparticles for removal of fluoride from aqueous solution through adsorption has been investigated. All the experiments were carried out by batch mode. The effect of various parameters viz. contact time, pH effect (pH 2–10), adsorbent dose (0.01–0.1 g/100 ml), initial fluoride concentration (10–100 mg/l) and competitive ions has been investigated to determine the adsorption capacity of CaO nanoparticles. Almost complete removal (98%) of fluoride was obtained within 30 minutes at an optimum adsorbent dose of 0.6 g/L for initial fluoride concentration of 100 mg/L. The adsorption isotherm was also studied to find the nature of adsorbate-adsorbent interaction.

Keywords: Adsorption, CaO nanoparticles, fluoride removal, sol-gel

INTRODUCTION

Recently, metal oxides have attracted much attention (1) because of their wide-ranging potential applications in catalysis, adsorption and nano-technology. Materials with nanodimension have attracted considerable

Received 19 November 2008; accepted 20 April 2009.
Address correspondence to Shobhana Menon, Department of Chemistry, School of Sciences, Gujarat University, Ahmedabad 380009, Gujarat, India. Tel.: +91 79 26302286; Fax: +91 79 26308545. E-mail: shobhanamenon07@gmail.com

attention because of their usefulness as sensors, as coating materials, and for the miniaturization of devices. Nanocrystalline alkaline earth metal oxides attract significant attention as effective chemisorbents for toxic gases, HCl, chlorinated, and phosphorus containing compounds (2). Therefore, high surface area materials, having the maximum number of defect sites/unit area, should be of interest as destructive adsorbent (3). Among the several route to prepare metal oxide nanoparticles, the sol-gel technique is well known to provide finely pure and homogeneous particles. The sol-gel method is based on inorganic polymerization reactions. The sol-gel process includes four steps—hydrolysis, polycondensation, drying, and thermal-decomposition. Considerable efforts have been made for the development of synthetic approaches of metal oxide nanoparticles before (1,4,5). We report simple and effective sol-gel route for synthesis of homogeneous and narrow size distributed calcium oxide nanoparticles using ethylene glycol and citric acid without any critical conditions like pH adjustment, surfactants, controlled heating rate, etc. The related characteristics of the prepared CaO crystalline powder samples have been investigated using Transmission Electron Microscope (TEM), FT-IR transmission, and thermal analysis (TG-DTA).

Fluoride-related health hazards are a major environmental problem in many regions of the world. As per the WHO standards for drinking water recommended a desirable limit of 1.0 mg/L and a permissible limit of fluoride is 1.5 mg/L. When the fluoride concentration is more than the permissible limit, it causes dental and skeletal fluorosis, bone diseases, mottling of teeth, lesions of the thyroid, liver, and other organs (6). Various treatment and technologies, based on the principle of precipitation, ion exchange, electrolysis, membrane, and adsorption have been proposed and are tested for the removal of excess of fluoride from drinking water as well as from industrial effluent (7–10). Among these methods, adsorption is the most widely used method for the removal of fluoride from aqueous solution. Several materials have been utilized for the removal of fluoride from aqueous solution by adsorption and precipitation processes, such as activated alumina (11), amorphous alumina (12), activated carbon (13), zeolite (14), hydrotalcite-like compounds (15), etc. In recent years, considerable attention has been given to the study of different types of low-cost materials such as calcite, clay charcoal, tree bark, saw dust, rice husk, and ground nut husk (16–19). However, the lowest limit for fluoride reduction by most of the adsorbents is greater than 2 mg/l with low adsorption capacity and high equilibrium time therefore, they are not suitable for the drinking water treatment purpose, especially as some of them can only work at an extreme pH value, such as activated carbon which is only effective for fluoride removal at pH less than 3.0 (20).

Calcium metal has a good affinity to fluoride ion. Much research has been done for the removal of fluoride by different calcium salt (21–25). But, the most important factors influencing the adsorption are the pH of water, the high adsorption capacity, and the crystalline form of the adsorbent, which was not satisfying by the previously reported method, therefore a new method for fluoride removal by calcium metal is highly desirable. Nanoparticles have unique adsorption properties due to their small size and large surface area, and hence in the present study, an attempt has been made to take a simple route to prepare CaO nanoparticles which could be a cheap and efficient adsorbent for fluoride removal. The present study deals with the kinetic and mechanistic aspects of fluoride removal using CaO nanoparticles.

EXPERIMENTAL

Synthesis of CaO Nanoparticles

A sol–gel method was developed to synthesize CaO nanoparticles in this study. All the starting materials for the synthesis used were of analytical grade. Calcium nitrate tetrahydrate (5.0 g) (Pfizer) was dissolved in 1 M aqueous solution of ethylene glycol (100 ml) into which 50 ml citric acid (0.9 g) solution in deionized water (Millipore-Q) was added dropwise with continuous stirring. Traditionally, the chelating agent provides the mixing of cations at the molecular level in a sol–gel process, but here citric acid is used as a carbon source to prepare the polymerized gel. The mixture was heated gently at 60–80°C for 2 h under stirring and was then further heated at 120°C to yield the polymeric gel. The gel precursor so formed was decomposed at 350° for 3 h and subsequently calcinated at 400°, 550°, 700°, 800°, and 900°C for 2 h in air and slowly cooled in a furnace to obtain white CaO nanoparticles.

The FT-IR of the gel and calcinated powders are recorded from 4000 to 400 cm^{-1} by the KBr pellet method using FT-IR Bruker Tensor 27 model. The TGA and DTA curves of dried gel are recorded using TGA-50 and DTA-60 Shimadzu respectively, up to 1000°C, at a heating rate of 10°C/min. TEM was obtained using a ZEISS EM-900 at the 85,000 magnification.

Defluorination

Stock solution of fluoride was prepared by dissolving 2.21 g of sodium fluoride (Merck, Germany) in 1 L deionized water (Millipore). The

measuring cylinder, the volumetric flask, and the conical flask used were of PVC. The pH measurements were made by a Systronics digital pH meter using a combined glass electrode. The pH meter was calibrated with Merck Standard buffers before any measurement. The required concentration of the fluoride solution was prepared by serial dilution of 1000 mg/L fluoride solution. The fluoride adsorption experiments from its aqueous solution on CaO nanoparticles were carried out using standard 100 mg/L fluoride solution in absence of any other competing ions. The adsorption experiments were carried out by adding 0.01 – 0.10 g of adsorbent in 100 ml of synthetic fluoride solution in 250 ml PVC flask covered with a glass dish. A glass dish was provided to avoid change in concentration due to evaporation. All the experiments were carried out at ambient temperature ($25 \pm 1°C$). After continuous stirring in a magnetic stirrer (Remi Equipments, Mumbai, India) at about 400 rpm for a predetermined time interval, the solid was separated by centrifugation (model no. R-4C, Remi laboratory centrifuge) (3000 rpm) and filtration through IC Millex-LG filter (Millipore) and the unadsorbed fluoride was estimated by Dionex ion chromatography system ICS 1000. Operating conditions were as follows: column, IonPac® AS-11 HC (4×250 mm); suppressor conductivity ASRS® ULTRA II 4-mm Anion self-regenerating Suppressor (ASRS); eluent, 20 mM sodium hydroxide (Sigma-Aldrich); column temperature $25 \pm 2°C$; flow rate 1.5 ml/min; injection volume, 25 µl; system backpressure 1920 psi; and background conductivity: 22 μS. The fluoride peak was observed at the retention time of 1.73 min. Each removal experiment was conducted twice to obtain reproducible results with an error of less than 5%, more test runs were conducted as required. The analytical results could be reproduced with an accuracy of greater than 95%. The experimental parameters studied are adsorbent concentration, contact time, initial fluoride concentration, pH, temperature, and competitive anion concentrations (synthetic solutions of nitrate, sulphate, and phosphate).

RESULTS AND DISCUSSIONS

Characterization

Drying of gels is considered as a very important intermediate stage in synthesizing oxide nanoparticles. The characterization of the precursor gel allows controlling and understanding better the whole process of synthesis.

Figure 1 shows the FTIR spectra associated with the stretching and bending vibrations from 4000–400 cm^{-1} of the gel precursor and its

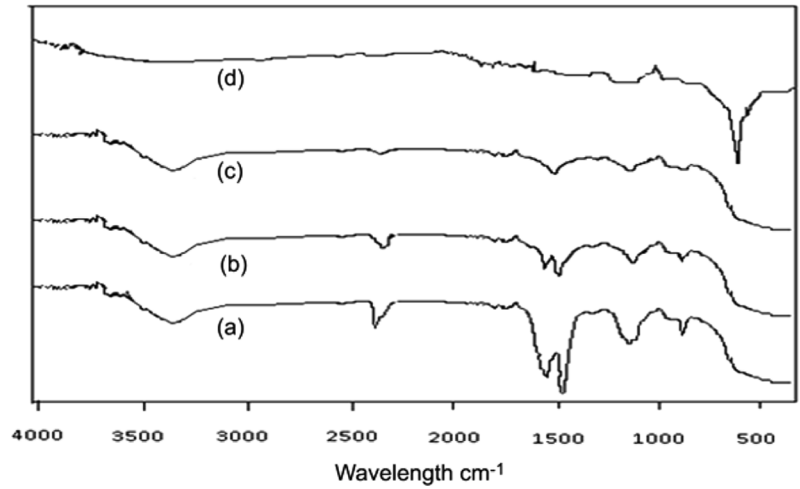

Figure 1. IR spectra of CaO nanoparticles at various temperatures: prepared by sol gel method (a) dried gel (b) 350°C (c) 550°C (d) 900°C.

decomposition products at various temperatures. After heating at 900°C, the band at 3400 cm^{-1} and 880 cm^{-1} in gel [Fig. 1(a)] is due to OH^- and H_2O vibration. This band [Fig. 1(d)] disappears after calcinations. The band at 1385 cm^{-1} and 1490 cm^{-1} in gel corresponds to the presence of NO_3^{-2}ions, which disappear at a higher temperature. A sharp band around 600 cm^{-1}[Fig. 1(d)], related to the formed metal-oxygen stretching, appeared which sharpens at higher sintering temperature.

To have more understanding of the CaO forming mechanism from the gel to the oxide nanoparticles obtained by the chelate gel route, the gel was thermally analyzed and the resultant TGA and DTA curves are shown in Figs. 2(a) and (b), respectively. During heat treatment of the gel, several processes such as dehydration, oxidation of the residual organic groups, decomposition, and sintering took place. Figure 2 shows the TG and DTA curves of CaO dried gel precursor. In the DTA curve we observed an endothermic peak at 72°C, which is due to evaporation of water and an exothermic peak at 860°C due to the combustion of organic substances. The TGA plot for the gel precursor obtained from the developed process is shown in Figure 2(a). The TGA curve shows constant weight loss due to decomposition of the gel and combustion of organic substances (26,27). This leads to homogeneous distributed oxides.

TEM samples were prepared by depositing a drop of dispersed CaO nanoparticles in ethanol on the Formvar-coated copper grids (200 mesh), and the electron microscope was operated at 100 keV. Figure 3 shows

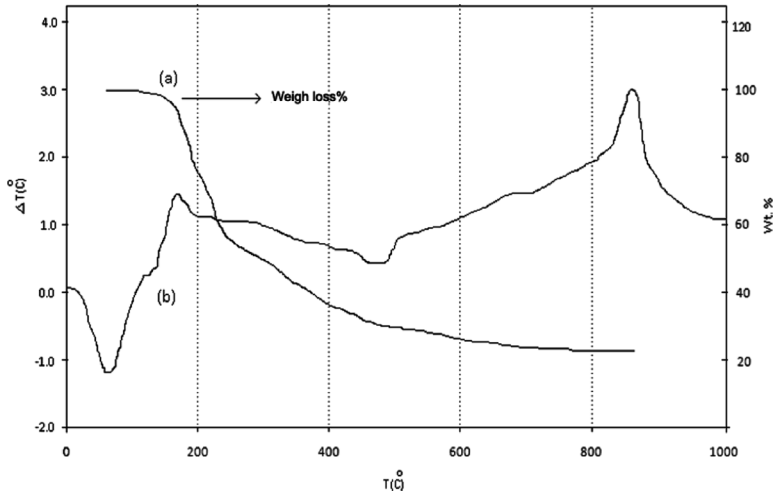

Figure 2. (a) TGA curves of dried gel. (b) DTA curve of synthesized gel at the heating rate of 10°C min^{-1}.

the transmission electron micrograph of the CaO nanoparticles. The averaged particle diameter obtained from TEM electromicrographs is less than 15.0 nm.

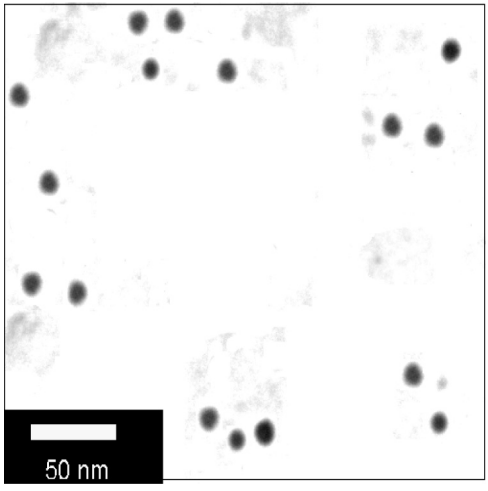

Figure 3. Transmission electron microscope image of CaO nanoparticles.

Effect of Adsorbent Dose

The effect of the adsorbent dose on the removal of fluoride was studied at ambient temperature ($25 \pm 2°C$) and contact time of 30 min for initial fluoride concentration of 100 mg/L. The results are presented with a scatter chart in Fig. 4. It is evident from this Figure that the removal of fluoride increased from 21.2% to 98.0% for 0.01–0.06 g/100 ml of CaO (initial fluoride concentration of 100 mg/L). Therefore the capacity of the adsorbent is 163333 mg/Kg.

A distribution coefficient K_D which reflects the binding ability of the surface for fluoride mainly depends on the type of adsorbent surface. The distribution coefficient K_D for fluoride was calculated according to the following equation: (28)

$$K_D = C_s/C_w(L/g) \quad (1)$$

where, C_s is the concentration of fluoride in the solid particles (mg/g) and C_w is fluoride concentration in aqueous solution (mg/L). The concentration of fluoride in the solid phase was calculated based on measurement of fluoride in the water before and after the adsorption of fluoride on the solid phase. It is seen from the results (not shown) that the distribution coefficient K_D increases with an increase in nanoparticles concentration, indicating the homogeneous nature of the surface of the adsorbent.

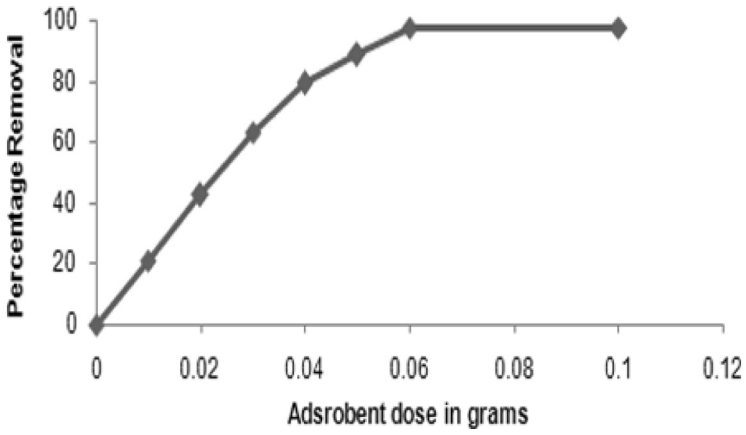

Figure 4. Adsorbent dose vs. percentage removal of fluoride (Initial concentration = 100 mg/L; adsorbent dose = 0.6 g/L; temperature = $25 \pm 1°C$; contact time = 30 min).

Effect of Contact Time

The percentage of fluoride adsorbed for initial fluoride concentration of 100 mg/L keeping other parameter constant, is presented in Fig. 5. It is evident that the adsorption process is very fast and most of the fluoride ion is adsorbed in the first 15 min and equilibrium was established, almost after 30 min. The change in the rate of removal might be due to the fact that initially all adsorbent sites were vacant and the solute concentration gradient was high. Later, the fluoride uptake rate by adsorbent was decreased significantly, due to the decrease in the number of adsorption sites as well as fluoride concentration. Decreased removal rate, particularly, towards the end of the experiment, and the smooth removal curve indicates the possible monolayer formation of fluoride ion on the outer surface of adsorbent.

Adsorption Kinetics

Adsorption of fluoride ion was rapid for the first 15 min and its rate gradually slowed down as the equilibrium approached. The rate constant K_{ad} for the sorption of fluoride was studied by the pseudo-first order rate expression, popularly known as the Lagergren equation, is generally described by the following Eq. (2) (Lagergren, 1898) (28):

$$\log(q_e - q_t) = \log q_e - K_{ad}(t/2.303) \tag{2}$$

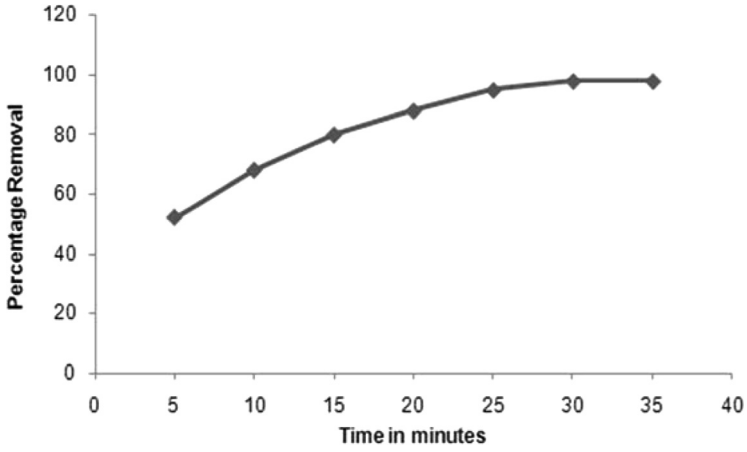

Figure 5. Time vs. percentage removal of fluoride (Initial concentration = 100 mg/L; adsorbent dose = 0.6 g/L; temperature $25 \pm 1^{\circ}C$).

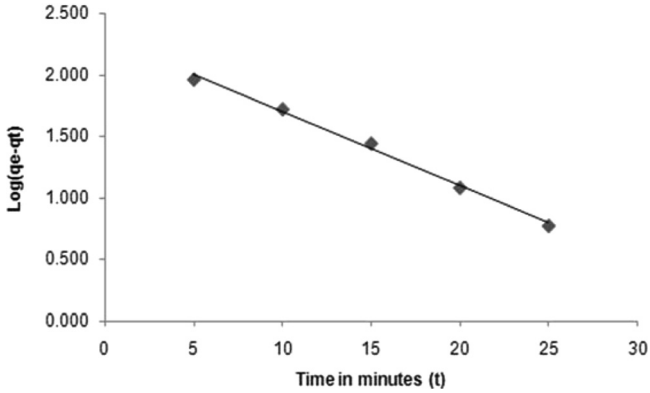

Figure 6. Adsorption kintetics, time vs. log ($q_e - q_t$) (Initial concentration = 100 mg/L; adsorbent dose = 0.6 g/L; temperature 25 ± 1°C).

where, q_e is the amount of fluoride adsorbed at equilibrium per unit weight of adsorbent (mg/g); q_t is the amount of fluoride adsorbed at any time (mg/g). The straight line plot of log ($q_e - q_t$) versus 't' with $r^2 > 0.99$, indicates the validity of the Lagergren equation of first-order kinetics (Fig. 6). The adsorption rate constant (K_{ad}) is calculated from the slope of the above plot and was found to be $5.5 \times 10^{-2}\,min^{-1}$ for initial fluoride concentration of 100 mg/L under experimental condition. The pseudo-second order rate expression generally applied to heterogeneous materials, which is not the case of this study (15).

Effect of Temperature

The effect of temperature on the adsorption of fluoride with initial concentration 100 mg/L was studied using optimum adsorbent dose (0.06 g/100 mL). A little adverse effect was observed on the adsorption of fluoride. The results are represented as percentage removal of fluoride versus temperature (Fig. 7). The percentage removal of fluoride with initial concentration decreased from 98.0% to 89.0% for 298–353 K temperature, even though the fluoride adsorption at a given temperature increased with time. This may be happening because the rise in temperature increases the escaping tendency of the molecules from interface and thereby diminishes the extent of adsorption. However, it is seen from observations that the decrease in percentage removal is not that large.

This was further supported by calculating thermodynamic parameters such as change in free energy (ΔG°), enthalpy (ΔH) and entropy

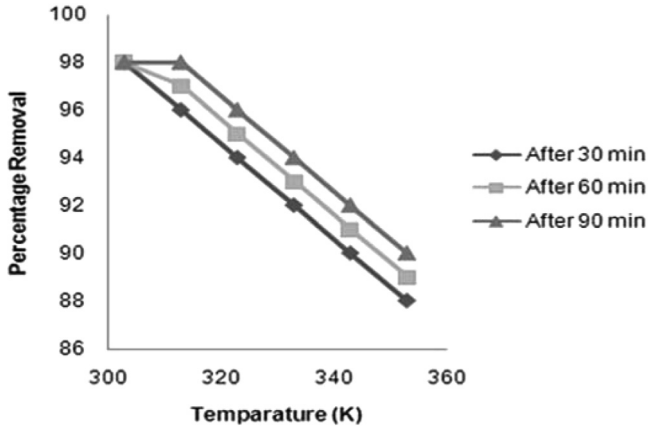

Figure 7. Temparature (K) vs. percentage removal of fluoride (Initial concentration = 100 mg/L; adsorbent dose = 0.6 g/L).

(ΔS) of adsorption were calculated using the following equations which determined using this equation (29):

$$\ln K_D = \Delta S/R - \Delta H/RT$$
$$\Delta G = \Delta H - T\Delta S \quad (3)$$

where, ΔS and ΔH are the changes in entropy and enthalpy of adsorption, respectively, which was evaluated from the slope and intercept of van't Hoff plots ($\ln K_D$ vs. 1/T) respectively and is represented in Table 1. The positive value of entropy (ΔS) indicates an increase in the randomness of the ongoing process and hence a good affinity of fluoride with CaO nanoparticles. The negative value of ΔG at each temperature indicates the feasibility and spontaneity of the ongoing adsorption.

Table 1. Thermodynamic parameters using synthetic fluoride solution of 100 mg/L

Temp (K)	ΔH (J/mol)	ΔS (J/K mol)	−ΔG (KJ/mol)
303	0.009	0.011	3.324
313			3.434
323			3.544

Effect of Initial Fluoride Concentration

The adsorption of fluoride onto CaO nanoparticles was studied by varying the initial fluoride concentration using an optimum adsorbent dose (0.06 g/100 mL) at ambient temperature ($25 \pm 2^{\circ}C$) for a contact time of 30 min. The results are represented in graphical form as percentage removal versus initial fluoride concentration in Fig. 8. The initial fluoride concentration was increased from 100 to 500 mg/L and the corresponding removal achieved a maximum value of 98.0% (initial concentration of 100 mg/L) and then it is gradually decreased to 55.8% (initial concentration of 500 mg/L). However, it is clear from Fig. 8 that, the maximum removal takes place when the initial concentration is low (i.e., 100 mg/L) and the removal is very less at high concentrations. This suggests the need of a high adsorbent dose to reduce the residual fluoride to a permissible level.

Adsorption Isotherm

The adsorption isotherm is the very first and significant parameter of adsorption studies because the shape of the adsorption isotherm not only provides a quantitative relationship between the adsorbed amount and equilibrium concentration of adsorbate, but also reflects the manner in which the adsorbate molecules are adsorbed on the surface of the adsorbent.

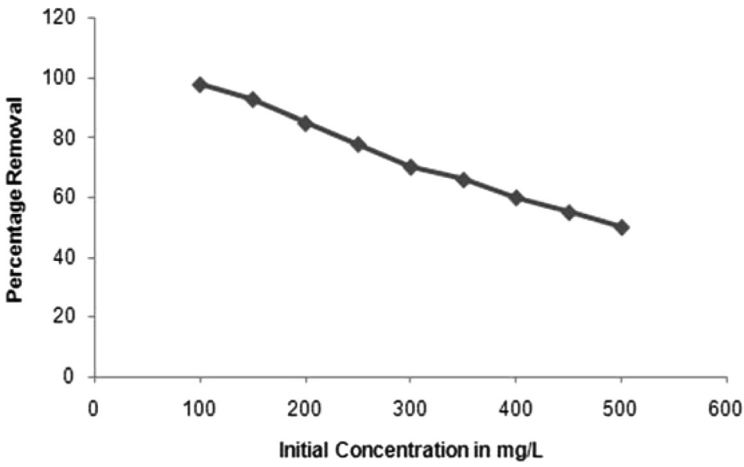

Figure 8. Initial fluoride concentration vs. percentage removal (Adsorbent dose = 0.6 g/L; temperature $25 \pm 1^{\circ}C$; contact time = 30 min).

To model the present process, the equilibrium data was fitted to Fruendlich, Langmuir, and Dubinin-Radushkevich (D–R) isotherm. The linearized Freundlich adsorption isotherm can be written as:

$$\log q_e = \log K_f + 1/n \log C_e \quad (4)$$

where, q_e is the adsorbed fluoride at equilibrium per unit mass of adsorbents (mg/g), K_f is the minimum sorption capacity (mg/g), and $1/n$ is the adsorption intensity. C_e is the equilibrium concentration of fluoride (mg/L). Figure 9 shows a plot of log q_e versus log C_e. The constants $1/n$ and log K_f values are obtained from the slope and intercept respectively. It is found that the related correlation coefficient R^2 value for the Freundlich model is 0.999. The Freundlich isotherm with minimum adsorption capacity of 21.33 mg/g of the adsorbent and adsorption intensity is 0.996. The intensity value <1 indicates the favorable situation. The experimental data fit well to the Freundlich isotherm model and validate the adsorption occurring on the homogeneous surfaces (28).

The linearized Langmuir equation, which is valid for monolayer sorption onto a surface with a finite number of identical sites, is written as (29):

$$1/q_e = 1/q_o b C_e + 1/q_o \quad (5)$$

where, q_o is the maximum amount of the fluoride ion per weight of the CaO nanoparticles to form a complete monolayer on the surface

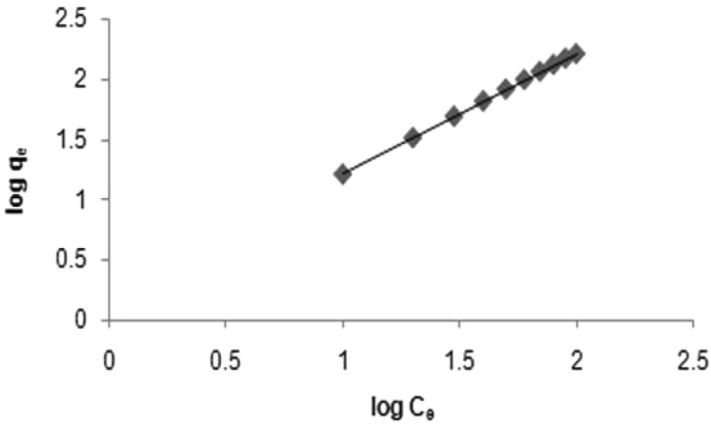

Figure 9. Linearized Freundlich adsorption isotherm, logC_e vs. logq_e (Adsorbent dose = 0.6 g/L; temperature = 25 ± 1°C; contact time = 30 min).

(adsorption capacity), C_e denotes the equilibrium adsorbate concentration in solution, q_e is the amount adsorbed per unit mass of the adsorbent, and b is the binding energy constant. The linear plot of $1/C_e$ versus $1/q_e$ (Fig. 10) indicates the applicability of Langmuir adsorption isotherm. The values of Langmuir parameters, q_o and b are 163.3 mg/g and 0.043 L/mg, respectively.

In order to predict the adsorption efficiency of the adsorption process, the dimensionless equilibrium parameter was determined by using the following equation:

$$R = 1/1 + bC_o \tag{6}$$

where b is the Langmuir constant and C_o is the initial adsorbate concentration (mg/L), the R value indicates that the type of isotherm be irreversible ($R = 0$), favorable ($0 < R < 1$), linear ($R = 1$), or unfavorable ($R > 1$). The R-value for the initial concentration of 100 mg/L was found to be 0.699. The value indicated a favorable system (30).

It is known that the Langmuir and Freundlich adsorption isotherm constant do not give any idea about the adsorption mechanism. In order to understand the adsorption type, equilibrium data were tested with Dubinin–Radushkevich (DR) isotherm (30). The linearized DR equation can be written as:

$$\ln q_e = \ln q_m - K\varepsilon^2 \tag{7}$$

where, ε is the Polanyi potential, and is equal to $RT \ln(1 + 1/C_e)$, q_e the amount of the fluoride adsorbed per unit mass of the adsorbent, q_m the

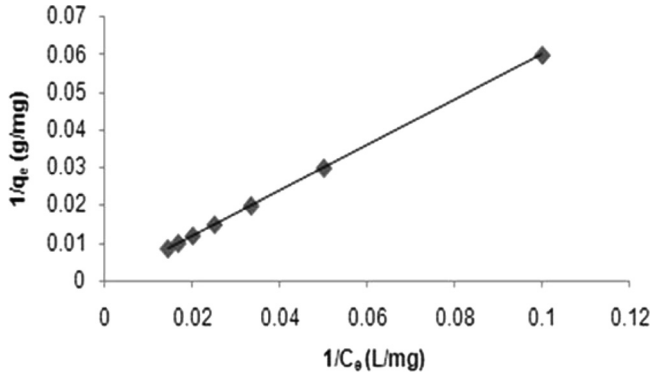

Figure 10. Langmuir adsorption isotherm $1/C_e$ vs. $1/q_e$ (Adsorbent dose = 0.6 g/L; temperature = 25 ± 1°C; contact time = 30 min).

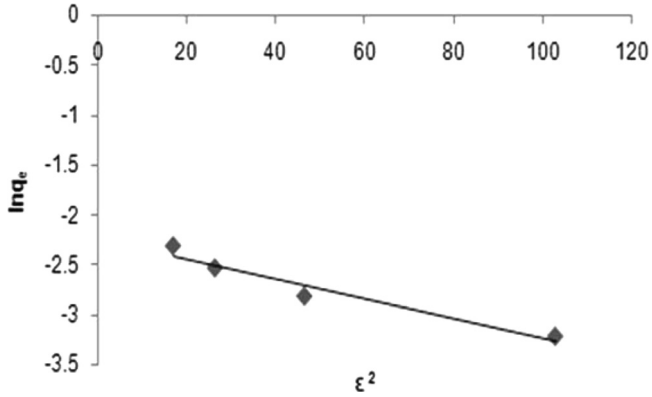

Figure 11. DR adsorption isotherm, ln q_e vs. ε^2 (Adsorbent dose = 0.6 g/L; temperature = 25 ± 1°C; contact time = 30 min).

theoretical adsorption capacity, C_e the equilibrium concentration of fluoride, K the constant related to adsorption energy, R the universal gas constant, and T is the temperature in K. Figure 11 shows the plot of $\ln q_e$ against ε^2, which was almost linear with correlation coefficient, $r^2 = 0.944$. DR isotherm constant K was calculated from the slope of the plot. The value of K was found to be $-2.0 \times 10^{-3}\,mol^2\,kJ^{-2}$.

The mean free energy of adsorption (E) was calculated from the constant K using the relation (31):

$$E = (-2K)^{-1/2} \tag{8}$$

It is defined as the free energy change when 1 mol of ion is transferred to the surface of the solid from infinity in solution. The value of E was found to be $15.76\,kJ\,mol^{-1}$. The value of E is very useful in estimating the type of adsorption and if the value is less than $8\,kJ\,mol^{-1}$, then the adsorption is physical in nature and if it is in between 8 and $16\,kJ\,mol^{-1}$, then the adsorption is due to the exchange of ions. (32) The value found in the present study was in between 8 and $16\,kJ\,mol^{-1}$ so the adsorption can be best explained as an exchange of ions.

Mechanism of Surface Adsorption

When CaO nanoparticles are added to water, it is converted into calcium hydroxide immediately and there is an adsorption of fluoride occurring by surface chemical reaction, in which hydroxide ions of calcium hydroxide are replaced rapidly by fluoride ions with the

formation of CaF_2. Both of the above processes can be represented by the following equation:

$$CaO + H_2O \longrightarrow Ca(OH)_2 + H^+$$
$$Ca(OH)_2 + 2F^- \longrightarrow CaF_{2(s)} + 2OH^- \quad (9)$$

Many researchers (21–25) have used various forms of lime [$Ca(OH)_2$, CaO, $CaCO_3$] or other calcium salts to increase the calcium activity in solution, thereby removing fluoride by precipitation as fluorite (CaF_2). Comparatively all of the above adsorbents are given a lower adsorbent capacity against CaO nanoparticles because the particle size of the CaO nanoparticles is very small and a large surface area. The amount of fluoride removed is dependent on the particle size and the surface area of the adsorbent (19). A decrease of the particle size to the nanometer range results in an increase of the dispersion (i.e., exposed surface area), which in turn, increases the adsorption capacity and diminishes the adsorbent volume. TEM micrographs of CaO nanoparticles before and after adsorption are presented in Figs. 12(a) and (b). The TEM micrograph clearly shows the surface modification.

Effect of pH

The most important single factor that controls the adsorption of ions on the oxide surface is the pH of the aqueous solution. In basic (>8 pH) adsorbate medium, the fluoride removal efficiency and capacity of

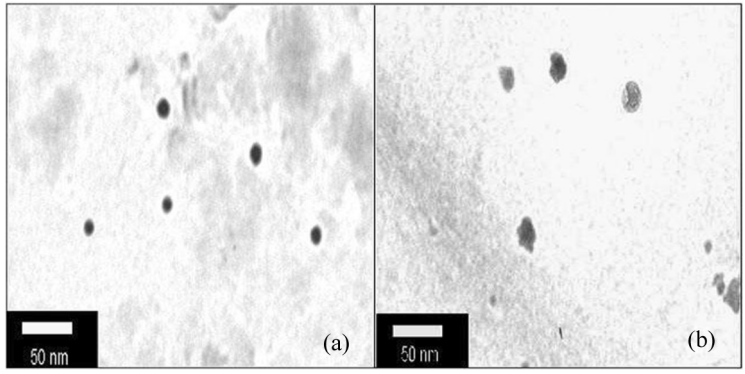

Figure 12. TEM images of CaO nanoparticles (a) before and (b) after fluoride adsorption Note: some shape variation occurred on CaO nanoparticles after adsorption of fluoride.

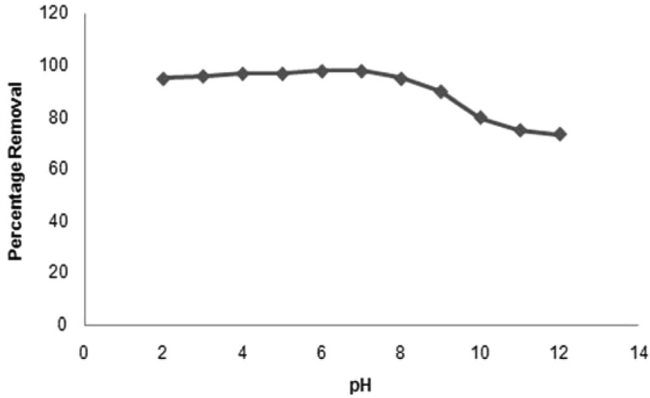

Figure 13. pH vs. percentage removal of fluoride (Initial concentration = 100 mg/L; adsorbent dose = 0.6 g/L; temperature = 25 ± 1°C; contact time = 30 min).

the adsorbent decreased. The progressive decrease (Fig. 13) of fluoride uptake at pH > 8 is possibly due to the electrostatic repulsion of fluoride ion to the negatively charged surface and the competition for active sites by an excessive amount of hydroxyl ions (33). It is apparent that the percentage of fluoride removal remains nearly constant at the lower pH (2–8). Since anion adsorption is coupled with a release of OH^- ion, the adsorption of the fluoride on the particle surface is probably favored in low pH. The fluoride uptake capacity of the solution is not much affected in the pH range less than or equal to 8, possibly due to the presence of positively charged and neutral sites at the surface of the adsorbent.

Effect of Competitive Ions

Drinking water and wastewater contains many anions. Therefore, it was thought worthwhile to study the effect of competitive ions like sulphate, nitrate, and phosphate on the adsorption of fluoride. Varying concentration of these solutions was prepared from their potassium salts (Merck). The initial concentration of fluoride was fixed at 100 mg/L while the initial concentrations of other anions varied from 100 to 500 mg/L and added individually and mix in the solution. The result of these studies is given in Figs. 14(a) and (b). It is clear from the figure that the adsorption capacity for fluoride decreased nominal (<2%) in the case of the highest concentration 500 mg/L of other competitive ions. Figure 14b is the chromatogram of the mixture of ions. This indicates that the adsorption of fluoride is not adversely affected by the presence of other ions in solution.

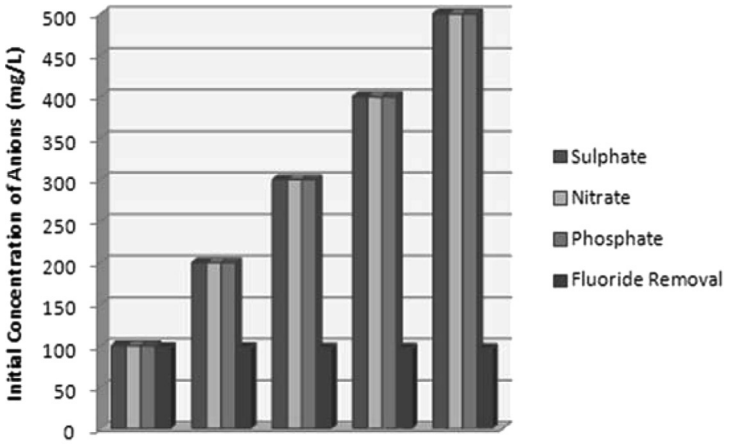

(a)

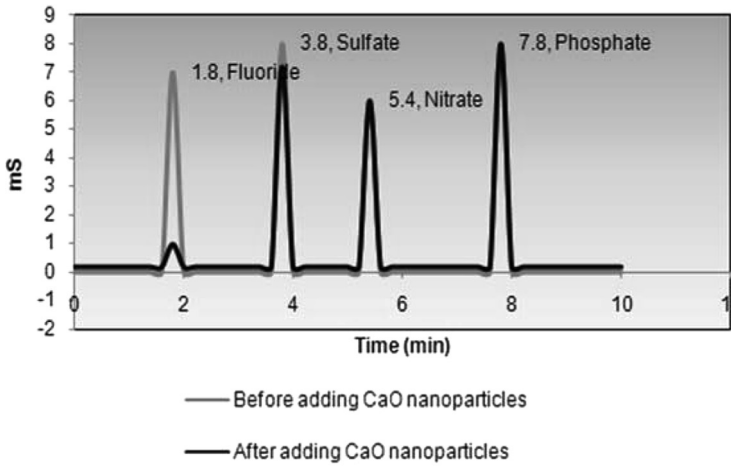

(b)

Figure 14. Effect of competitive ions (Sulphate, Nitrate and Phosphate) with target fluoride ion (b) Chromatogram of the mixture of competitive ions and fluoride (Initial concentration = 100 mg/L; adsorbent dose = 0.6 g/L; temperature = $25 \pm 1^{\circ}C$; contact time = 30 min).

Desorption Study

To make a cost-effective and user-friendly process, the adsorbent should be regenerated, so as to reuse for further fluoride adsorption. Desorption studies were carried out by using the fluoride adsorbed

Table 2. Comparison of the present method with other reported method

Adsorbent	Capacity (mg/Kg)
Activated alumina (11)	1450
Amorphous alumina supported corbon nanotube (12)	14900
Zeolite (14)	391
Hydrotalcite like Compounds (15)	1202
Soil (16)	150
Carbon nanotube (34)	3000
Rare earth oxide (35)	123
Present method (CaO nanoparticles)	163333

adsorbent. First, the fluoride-adsorbed CaO nanoparticles are generated by adsorbing 100 mg/l fluoride solution on 0.06 g/l at pH 6.5. After the equilibration, the residue was filtered and the filtrate was measured for fluoride content. Then this fluoride-adsorbed CaO nanoparticles were subjected for desorption studies by maintaining the pH values (2–12) by addition of 0.1 M NaOH or 0.1 M HCl solution in each flask and the suspensions were conditioning for 30 min at 50 rpm. The process of adsorption is predominantly chemical in nature. So, desorption of the adsorbed fluoride on adsorbent resulted only about 50%

Comparison with Other Adsorbents

The capacity of novel CaO nanomaterial was found to be much higher than many of the adsorbents reported recently (Table 2).

CONCLUSIONS

A novel material, CaO nanoparticles was prepared. The results of TEM and TGA-DTA indicate that particles are homogeneous and in nanometer size. The following conclusions may be drawn:

1. The kinetic study shows that the removal of fluoride was found to be very rapid during the initial period, i.e., most of the fluoride was removed in the first 15 min and reached a maximum of 98% at 30 min.
2. The adsorption followed first-order rate kinetics, and data fit into the linear form of the Freundlich, Langmuir, and Dubinin-Radushkevich (DR) isotherm models.

3. Other ions such as sulphate, nitrate, and phosphate up to 500 mg/L did not affect the adsorption of fluoride thereby indicating that the calcium oxide nanoparticles are a selective adsorbent for fluoride. Higher adsorption capacity of CaO nanoparticles makes them have great potential application in fluoride removal from water.

ACKNOWLEDGEMENTS

Financial assistance from UGC, New Delhi is gratefully acknowledged.

REFERENCES

1. Rao, C.N.R.; Vivekchand, S.R.C.; Biswasa, K.; Govindaraja, B. (2007) Synthesis of inorganic nanomaterials. *Dalton Trans.*, 3728–3749.
2. Mishakov, I.V.; Bedilo, A.F.; Richards, R.M.; Chesnokov, V.V.; Volodin, A.M.; Zaikovskii, V.I.; Buyanov, R.A.; Klabunde, K.J. (2002) Nanocrystalline MgO as a dehydrohalogenation catalyst. *J. Catalysis.*, *206*: 40.
3. Li, Y.X.; Klabunde, K.J. (1991) Nano-scale metal oxide particles as chemical reagents. Destructive adsorption of a chemical agent simulant, dimethyl methylphosphonate, on heat-treated agnesium oxide. *Langmuir.*, *7*: 1388.
4. Chu, S.Y.; Yan, T.M.; Chen, S.L. (2000) Characteristics of sol-gel synthesis of ZnO-based powders. *J. Mat. Sci. Lett.*, *19*: 349–352.
5. Kim, Y.T.; Young, P.S.; Heejoon, M.; Hee, C.K. (2008) A chelate-assisted route to anatase TiO_2 nanoparticles in acidic aqueous media. *Colloids and Surfaces A.*, *313–314*: 260–263.
6. Diesendorf, M.; Colquhoun, J.; Spittle, B. (1998) Fluoridation and bones: Author's response to crictics. *Fluoride.*, *31*: 166–169.
7. Nawlakhe, W.G.; Kulkarni, D.W.; Pathak, B.N.; Bulusu, K.R. (1975) Defluoridation of water by Nalgonda technique. *Indian J. Environ. Health.*, *17*: 26.
8. Yang, M.; Zhang, Y.; Shao, B.; Qi, R.; Myoga, H. (2001) Precipitative removal of fluoride from electronics wastewater. *J. Environ. Eng.*, *37*: 902.
9. Ku, Y.; Choi, H.M.; Wang, W. (2002) The removal of fluoride ion from aqueous solution by a cation synthetic resin. *Sep. Sci. Technol.*, *37*: 89–103.
10. Hichour, M.; Persia, F.; Sandeaux, J.; Gavachi, C. (2003) Modelisation of fluoride removal in Donnan dialysis. *J. Membr. Sci.*, *212*: 113–121.
11. Ghorai, S.; Pant, K.K. (2004) Investigations on the column performance of fluoride adsorption by activated alumina in a fixed-bed. *Chem. Eng. J.*, *98*: 165–173.
12. Li, Y.H.; Wang, S.; Cao, A.; Zhao, D.; Zhang, X.; Xu, C.; Luan, Z.; Ruan, D.; Liang, J.; Wu, D.; Wei, B. (2001) Adsorption of fluoride from water by amorphous alumina supported on carbon nanotubes. *Chem. Phys. Lett.*, *350*: 412–416.

13. Ramos, R.L.; Turrubiartes, J.O.; Castillo, M.A.S. (1999) Adsorption of fluoride from aqueous solution on aluminum-impregnated carbon. *Carbon.*, *37*: 609–617.
14. Samatya, S.; Yüksel, U.; Yüksel, M.; Kabay, N. (2007) Removal of fluoride from water by metal ions (Al^{3+}, La^{3+} and ZrO^{2+}) loaded natural zeolite. *Sep. Sci. Technol.*, *42*: 2033–2047.
15. Jiménez-Núñez, M.L.; Olguín, M.T.; Solache-Ríos, M. (2007) Fluoride removal from aqueous solutions by magnesium, nickel, and cobalt calcined hydrotalcite-like compounds. *Sep. Sci. Technol.*, *42*: 3623–3639.
16. Srimurali, M.; Pragathi, A.; Karthikeyan, J. (1998) A study on removal of fluorides from drinking water by adsorption onto low-cost materials. *Environ. Pollut.*, *99*: 285–289.
17. Reardon, E.J.; Wang, Y. (2001) Activation and regeneration of a soil sorbent for defluoridation of drinking water. *Appl. Geochem.*, *16*: 531–539.
18. Fan, X.; Parker, D.J.; Smith, M.D. (2003) Adsorption kinetics of fluoride on low cost materials. *Water Research.*, *37*: 4929–4937.
19. Turner, B.D.; Bining, P.; Stipp, S.L.S. (2005) Fluoride removal by calcite: Evidence for fluorite precipitation and surface adsorption. *Environ. Sci. Technol.*, *39*: 9561–9568.
20. McKee, R.H. (1984) Removal of flourides from drinking water. *Ind. Eng. Chem.*, *26*: 849–851.
21. Reardon, E.J.; Wang, Y.A. (2000) A limestone reactor for fluoride removal from wastewaters. *Environ. Sci. Technol.*, *34*: 3247–3253.
22. Simonsson, D. (1979) Reduction of fluoride by reaction with limestone particles in a fixed bed. *Ind. Eng. Chem. Process Des. Dev.*, *18*: 288–292.
23. Yang, M.; Hashimoto, T.; Hoshi, N.; Myoga, H. (1999) Fluoride removal in a fixed bed packed with granular calcite. *Water Research.*, *33*: 3395–3402.
24. Glover, E.D.; Sippel, R.F. (1962) Experimental pseudomorphs: replacement of calcite by fluorite. *Am. Mineral.*, *47*: 1156–1165.
25. Farrah, H.; Slavek, J.; Pickering, W.F. (1985) Fluoride sorption by soil components: calcium carbonate, humic acid, manganese dioxide and silica. *Aust. J. Soil Res.*, *23*: 429–439.
26. Temuujin, J.J.; Aoyama, M.; Senna, M.; Masuko, T.; Ando, C.; Kishi, H. (2004) Synthesis of Y-type hexaferrites via a soft mechanochemical route. *J. Solid State Chem.*, *177*: 3903–3908.
27. He, Z.; Ling, Q.Z. (2003) Kinetics and magnetic properties of sol–gel derived NiZn ferrite–SiO_2 composites. *Mater. Lett.*, *57*: 3031–3036.
28. Sujana, M.G.; Thakur, R.S.; Rao, S.B. (1998) Removal of fluoride from aqueous solution by using alum sludge. *J. Collo. Interf. Sci.*, *206*: 94–101.
29. Tahir, H. (2005) Comparative trace metal contents in sediments and liquid wastes from tanneries and the removal of chromium using ZEOLITE-5A. *EJEAF Chem.*, *4*: 1021–1032.
30. Hosseini, M.; Mertens, S.F.L.; Ghorbani, M.; Arshadi, M.R. (2003) Asymmetrical Schiff bases as inhibitors of mild steel corrosion in sulphuric acid media. *Mater. Chem. Phys.*, *78*: 800–809.

31. Namasivayam, C.; Yamuna, R.T. (1995) Adsorption of direct red 12 B by biogas residual slurry: Equilibrium and rate processes. *Environ. Pollut.*, *89*: 1–7.
32. Tahir, S.S.; Nassem, R. (2003) Thermodynamic studies of Ni(II) adsorption onto bentonite from aqueous solution. *J. Chem. Thermodyn.*, *35*: 2003–2009.
33. Nigussie, W.; Zewge, F.; Chandravanshi, B. (2007) Removal of excess fluoride from water using waste residue from alum manufacturing process. *J. Hazard. Mater.*, *147*: 954–963.
34. Li, Y.H.; Wang, S.; Zhang, X.; Wei, J.; Xu, C.; Luan, Z.; Wu, D. (2003) Adsorption of fluoride from aligned carbon nanotube. *Mat. Res. Bull.*, *38*: 469–476.
35. Raichur, A.M.; Jyoti Basu, M. (2001) Adsorption of fluoride onto mixed rare earth oxides. *Sep. Pur. Tech.*, *24*: 121–127.